Nanoscale

Accepted Manuscript

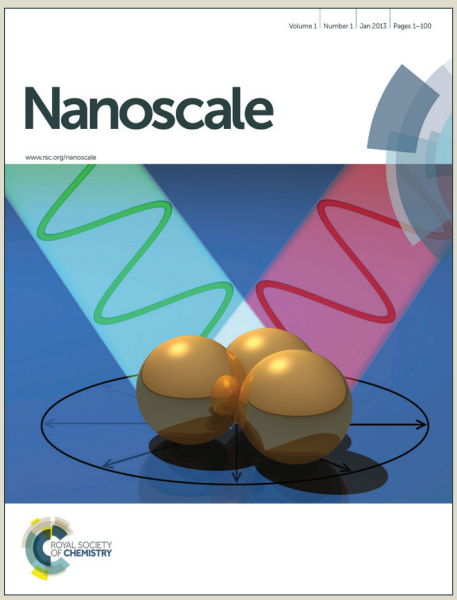

ROYAL SOCIETY OF CHEMISTRY

www.rsc.org/nanoscale

Thermal Conductivity of Zinc Blende and Wurtzite CdSe Nanostructures

Juekuan Yang,*[a] Hao Tang,[b,c] Yang Zhao,[a] Yin Zhang,[a] Jiapeng Li,[d] Zhonghua Ni,[a] Yunfei Chen,[a] and Dongyan Xu*[b,c]

[a] *School of Mechanical Engineering and Jiangsu Key Laboratory for Design and Manufacture of Micro-Nano Biomedical Instruments, Southeast University, Nanjing 211189, China*

[b] *Department of Mechanical and Automation Engineering, The Chinese University of Hong Kong, Shatin, New Territories, Hong Kong Special Administrative Region*

[c] *Shenzhen Research Institute, The Chinese University of Hong Kong, Shenzhen 518057, China*

[d] *School of Mechanical Engineering, Shandong University of Technology, Zibo 255049, China*

Email: yangjk@seu.edu.cn; dyxu@mae.cuhk.edu.hk

Abstract

Many binary octet compounds including CdSe can be grown in either wurtzite (WZ) or zinc blende (ZB) phase, which has aroused great interest among research community to understand the phase dependence of thermal transport properties of these compounds. So far, it is still debatable whether the ZB phase possesses higher thermal conductivity than the WZ phase. In this work, we report on thermal conductivity measurements of CdSe nanowires/nanoribbons with both WZ and ZB phases via a suspended device method. At room temperature, thermal conductivity

of all the ZB CdSe nanostructures measured in this work is higher than the bulk thermal conductivity of the WZ CdSe reported in the literature, suggesting that the bulk thermal conductivity of the ZB CdSe is higher than that of the WZ phase. Our result is different from previous experimental results in the literature for InAs nanowires which suggest similar thermal conductivity values for the bulk ZB and WZ InAs crystals. The higher thermal conductivity of the ZB CdSe can be explained by its lower anharmonicity and smaller number of atoms per unit cell compared to the WZ phase.

1. Introduction

Many binary compounds, such as AlN, InAs, GaAs, CdSe, SiC, etc., can be grown in two crystal phases, i.e., the WZ phase and the ZB phase, depending on the growth conditions.[1] This class of compounds has aroused great research interest to study the phase dependence of thermal transport properties. Zhou *et al*. measured thermal conductivity of the WZ and ZB InAs nanowires and their combined experimental and theoretical studies indicate that WZ and ZB phases of the bulk InAs possess similar thermal conductivity values.[2] Recently, it is predicted that thermal conductivity of the bulk ZB BeO could be 30% higher than that of the WZ phase at room temperature.[3] However, a recent work based on the linearized phonon Boltzmann equation from the first principle calculations (LBTE) claimed that the structural difference between ZB and WZ phases has little effect on lattice thermal conductivity of 33 compounds including both InAs and BeO.[4] It is also noticed that theoretical calculations in the literature gave conflicting results on the phase dependence of thermal conductivity for AlN. For example, AlShaikhi and Srivastava predicted that thermal conductivity of the ZB AlN is about 2.7 times that of the WZ phase at room temperature.[5] However, recent theoretical studies show no obvious phase dependence for thermal conductivity of AlN.[3, 4] Therefore, it is important to perform experimental studies to clarify the contradiction among theoretical calculations in the literature.

Unfortunately, for this class of compounds, bulk single crystalline samples usually

only exist in one phase, either ZB or WZ phase, due to the difficulty in synthesis. For example, bulk InAs crystals typically exhibit a ZB phase,[2] and CdSe has a preference to crystalize in the WZ phase when grown in bulk form.[6] However, recently, nanostructures of both phases have been successful synthesized for some of these compounds, which gives us an alternative opportunity to study the phase dependence of thermal conductivity using nanostructures.

In this work, we report on thermal conductivity measurements of single crystalline CdSe nanowires/nanoribbons with both ZB and WZ phases. CdSe is an important II-VI semiconductor and has attracted enormous attention due to its potential applications in transistors,[7] light emitting devices,[8, 9] solar cells,[10, 11] and lasers,[12] etc. Although many studies have been carried out on optoelectronic properties of CdSe,[8, 12-18] its thermal property is barely studied so far.[19-22] The bulk CdSe crystal is typically in the WZ phase. Thermal conductivity of the bulk WZ CdSe is reported to be 9 W/m-K at room temperature.[21, 22] Although the growth of the ZB CdSe epilayers has been demonstrated by molecular beam epitaxy,[23] thermal conductivity of the ZB CdSe has not been reported yet. Morelli and Slack theoretically calculated thermal conductivity of the bulk ZB CdSe to be 23 W/m-K at room temperature, which is about two times that of the WZ phase.[6] Togo *et al*. predicted a lattice thermal conductivity of 12.4 W/m-K for the bulk ZB CdSe and a value of 8.81 W/m-K for the bulk WZ CdSe at 300 K by using a LBTE model.[4] Consistent with theoretical predictions,[4, 6] our experimental results suggest that the bulk thermal

conductivity of the ZB CdSe is higher than that of the WZ CdSe reported in the literature at room temperature. Recently, a few researchers have reported thermal conductivity of nanostructured CdSe films. Feser *et al*. observed ultralow thermal conductivity in the range of 0.2 W/m-K to 0.43 W/m-K at 300 K for polycrystalline CdSe thin films depending on grain sizes.[21] Ong *et al*. found thermal conductivity of CdSe nanocrystal arrays to be less than 0.3 W/m-K at 300 K.[24] Ma *et al*. reported a thermal conductivity of 0.53 W/m-K for CdSe nanocomposites synthesized by solution-based processes.[25] The reported ultralow thermal conductivity in these works is mainly due to the existence of a large amount of grain boundaries or hard/soft interfaces in the nanostructured CdSe films.

2. Experimental

CdSe nanowires/nanoribbons with either ZB or WZ phase were synthesized in a Lindberg three-zone horizontal tube furnace via a vapor-liquid-solid (VLS) growth mechanism. CdSe powder (99.999%) was placed in the hot center of the tube furnace. Silicon wafers coated with 20 nm-in-diameter gold nanoparticles as catalysts were used as growth substrates, and were placed at the cold zone of the furnace which is 12 cm away from the center. The tube was initially pumped down to a base pressure of about 10^{-2} mbar. With the flow of 50 sccm argon gas, the hot center of the furnace was heated to 800 °C (for the ZB phase) or 850 °C (for the WZ phase) and then held at this temperature for about 45 mins with a pressure of 250-300 mbar (for the ZB phase) or 150-180 mbar (for the WZ phase). After that, the furnace

was naturally cooled down. A layer of CdSe nanowires/nanoribbons with either ZB or WZ phase was formed on the substrate. Figure 1 shows the high-resolution transmission electron microscopy (HRTEM) images and the corresponding Fourier transform diffraction patterns of a ZB CdSe nanowire (sample ZB1) and a WZ CdSe nanoribbon (sample WZ1) measured in this work. The growth direction is <110> for sample ZB1 and [001] for sample WZ1.

Thermal conductivity measurements were performed in a high-vacuum cryostat system with suspended microdevices that have been used to study thermophysical properties of various nanotubes,[26-28] nanoribbons,[29-31] and nanowires.[32, 33] The device consists of two adjacent suspended SiN_x membranes serving as a heat source and a heat sink, respectively. An individual CdSe nanowire can be picked up from the growth substrate by using a manipulator under an optical microscopy and aligned to bridge heat source and heat sink on a measurement device. In the vacuum chamber, two radiation shields were installed to reduce the radiation loss from the device to surroundings during the measurement so that it can be assumed that the temperature of each membrane is the same as the substrate temperature when the heating current is zero.[34] The temperature of the sample holder was calibrated using a silicon diode temperature sensor (Janis 670-HTCAL). The sensitivity of the sensor is ±0.1 K. A differential method with a bare reference device was used to cancel out the effect of the radiative heat transfer from the heat source to the heat sink on the measured thermal conductance of the sample.[35, 36] The details of the measurement

technique can be found elsewhere in the literature.[27, 35, 36]

3. Results and Discussion

3.1 ZB CdSe Nanostructures

Intrinsic thermal conductivity of three ZB CdSe nanowires was measured in this work by following a multiple-measurement approach in the literature.[31, 37] Table I summarizes the phase, lateral dimension(s), and growth direction for all the samples measured in this work. Figure 2(a)-(c) show the scanning electron microscopy (SEM) images of sample ZB1 measured with different suspended lengths. The diameter of sample ZB1 is 52 nm as listed in Table I. The sample was first measured with a suspended length (L_s) of 8.7 μm (Fig. 2(a)), then it was realigned and measured again with L_s = 3.7 μm (Fig. 2(b)). From these two measurements, the intrinsic thermal conductivity of sample ZB1 can be extracted assuming that contact thermal resistances between the nanowire and two membranes (R_{CM}) are same for these two measurements.[37] Figure 3(a) shows the calculated intrinsic thermal conductivity and effective thermal conductivity values obtained from two measurements, which include the contribution of R_{CM}. As expected, with the increase of the suspended length, the contribution of R_{CM} to the total thermal resistance decreases, and the obtained effective thermal conductivity increases. At 300 K, the effective thermal conductivity values obtained from L_s = 8.7 μm and 3.7 μm are 10.6 W/m-K and 9.3 W/m-K, respectively. The intrinsic thermal conductivity obtained from two measurements is 11.9 W/m-K, which is ~11% higher than the effective thermal conductivity obtained with L_s = 8.7 μm. It should be noted that the nanowire shown

in Fig. 2(b) is bent instead of straight as the one shown in Fig. 2(a). The bending length of the nanowire in Fig. 2(b) has been considered in the length calculation, which is directly measured from the SEM image by dividing the curved wire into many segments. We did not experimentally study the effect of bending on thermal conductivity of CdSe nanowires. It has been reported that bending has no obvious effect on thermal conductivity of carbon nanotubes and boron nitride nanotubes under severe structural deformation.[38] On the other hand, Liangruksa and Puri[39] theoretically predicted that surface stress could decrease the lattice thermal conductivity of a silicon nanowire. In this work, we neglected the effect of bending on thermal conductivity of sample ZB1 and assumed that intrinsic thermal conductivity is the same for two measurements in Fig. 2(a) and Fig. 2(b).

Assuming that R_{CM} is the same in two measurements with different suspended lengths, we can also extract R_{CM}, which is given in Fig. 3(b).[37] At 300 K, R_{CM} is determined to be 4.0×10^7 K/W, and the contact thermal resistance per unit length is estimated to be 10 m-K/W using the fin model.[37, 40] For the measurement with L_s = 8.7 μm, the ratio of R_{CM} to the measured total thermal resistance is maximum (~14.3%) at 100 K, and decreases to ~10.3% at 300 K. Due to the low ratio of R_{CM} to the total thermal resistance, the uncertainty in R_{CM} is estimated to be >35% in the whole measurement temperature range, and >50% above 300 K. Based on the fin model,[40] the required contact length between the nanowire and membranes for the nanowire to be fully thermalized can be calculated by $L_c = R_{CM}/R_{NW/L}$, where $R_{NW/L}$ is the intrinsic thermal

resistance of the CdSe nanowire per unit length. When the actual contact length is larger than L_c, R_{CM} will not depend on the contact length anymore. For sample ZB1, L_c is calculated to be 1.45 μm at 100 K and 1.0 μm at 300 K, which is less than the actual contact length as shown in Fig. 2(a) and 2(b), and therefore it is rational to assume that R_{CM} is the same in two measurements with different suspended lengths.

In a former study, we have shown that the deposition of a Pt-C composite at the contacts between the measured sample and two membranes can reduce the contact thermal resistance through increasing the contact area between the sample and the heat source/sink.[31] We also tried to deposit a Pt-C composite via electron-beam-induced deposition (EBID) at the contacts between the nanowire and two membranes after the second round measurement with L_s = 3.7 μm, as shown in Fig. 2(c). The obtained effective thermal conductivity as given in Fig. 3(a) increases significantly after the deposition of the Pt-C composite. The contact thermal resistance after the Pt-C deposition can be evaluated from the measured total thermal resistance of sample ZB1 with the Pt-C deposition and its intrinsic thermal conductivity, which is determined to be 1.3×10^7 K/W at 300 K and is only one third of the value obtained before the deposition. With the Pt-C deposition, in order to reduce the ratio of the contact thermal resistance to intrinsic thermal resistance of sample ZB1 to be <5% in the whole temperature range, L_s should be larger than 15 μm and it is expected to increase as the nanowire diameter increases. However, the largest gap between two membranes of our devices is only 6 μm, it is very difficult to

prepare samples with L_s >15 μm. Therefore, we choose to use multiple-measurement method below to measure the intrinsic thermal conductivity of other ZB nanowires (ZB2 and ZB3).

Intrinsic thermal conductivity of three ZB CdSe nanowires (ZB1, ZB2, and ZB3) is shown in Fig. 4(a) and the values at 300 K are also listed in Table I. The diameters of ZB2 and ZB3 are 41 nm and 88 nm, respectively. As shown in Fig. 4(a), thermal conductivity of CdSe nanowires decreases as the diameter is reduced presumably due to the enhanced phonon-boundary scattering. As seen in Table I, thermal conductivity values at 300 K are 10.6 W/m-K, 11.9 W/m-K, and 14.1 W/m-K for nanowires with a diameter of 41 nm, 52 nm, and 88 nm, respectively. The bulk thermal conductivity of CdSe with the WZ phase is reported to be 9 W/m-K at room temperature,[21, 22] which is lower than thermal conductivity values we obtained on all three ZB nanowires. This may be due to the structural difference in WZ and ZB phases.

Thermal conductivity measurement of the bulk CdSe with the ZB phase has not been reported so far. In order to estimate the bulk thermal conductivity of the ZB CdSe, we measured a CdSe nanoribbon with a relatively large cross section (sample ZB4), which is taken from the same growth substrate as other measured ZB nanowires. The width and thickness of sample ZB4 are 485 nm and 195 nm, respectively. The effective thermal conductivity of sample ZB4 measured with L_s = 9.4 μm is given in

Fig. 4(a). Since the thermal conductance of sample ZB4 is large due to its large cross section, during the measurement, the temperature difference between heat source and heat sink is small (less than 0.4 K in the whole measurement temperature range). Thus, compared with other thin ZB nanowires measured in this work, the same level of temperature fluctuation of heat source and heat sink can lead to a relatively large scatter in the measured effective thermal conductivity of sample ZB4. The scatter of effective thermal conductivity will increase as the suspended length decreases. Therefore, we did not attempt to shorten the suspended length to determine the intrinsic thermal conductivity of sample ZB4. Instead, we tried to estimate the contact thermal resistance between sample ZB4 and two membranes based on the R_{CM} value obtained on sample ZB1. As mentioned above, the contact thermal resistance per unit length is estimated as 10.0 m-K/W at 300 K for sample ZB1 by using the fin heat transfer model.[37, 40] The contact width between sample ZB1 and the membrane is calculated to be 1.38 nm by using a model for estimating the contact length of a cylinder in contact with a planar substrate in the literature.[41, 42] Assuming that the contact thermal resistance per unit area between the CdSe nanostructure and the membrane is a constant, the contact thermal resistance per unit length between sample ZB4 and the membrane can be evaluated to be 0.028 m-K/W at 300 K. Using the fin model again,[37, 40] contact thermal resistance between sample ZB4 and the membrane is estimated to be 2.5×10^5 K/W at 300 K, which is ~20 times smaller than the measured thermal resistance of sample ZB4. In the temperature range of 60 K to 360 K, the contribution of contact thermal resistance to the total

thermal resistance is less than 8% for sample ZB4.

As shown in Fig. 4(a), thermal conductivity of sample ZB4 only shows a slight decreasing trend above 150 K, which suggests that boundary scattering still plays a significant role even for a ZB nanoribbon with a width of 485 nm and a thickness of 195 nm. Considering that thermal conductivity of sample ZB4 at 300 K (18.8 W/m-K) is only slightly lower than the thermal conductivity of the bulk ZB CdSe predicted by Morelli and Slack (23 W/m-K)[6] and boundary scattering is still significant for this sample, we speculate that the bulk thermal conductivity of the ZB CdSe might be even higher than 23 W/m-K at 300 K. On the other hand, it has been reported that thermal conductivity of nanowires may depend on the growth direction.[3, 43] In this work, the growth direction of samples ZB1-ZB3 is <110>, while it is <100> for sample ZB4. Thermal conductivity of all measured ZB nanowires/nanoribbons with growth direction of either <110> or <100> is higher than that of the bulk WZ CdSe, clearly indicating that thermal conductivity of the bulk ZB CdSe crystal is higher than the bulk thermal conductivity of the WZ CdSe reported in the literature at room temperature.

The relative uncertainty of thermal conductance was evaluated using the Monte Carlo method,[40] which is ~5% for sample ZB4, and less than 2% for other ZB samples. The diameter of samples ZB1, ZB2, and ZB3 and the width of sample ZB4 were measured from the TEM images, and the error was estimated as 2 nm considering the

variation along the length direction. The thickness of sample ZB4 was measured using an atomic force microscopy (AFM), and the error was estimated conservatively as 5 nm. The suspended lengths of all the samples were measured from SEM images, and the error was estimated as 0.25 μm. Above 100 K, the uncertainty in thermal conductivity was evaluated to be 1.0 – 2.0 W/m-K for all the ZB samples by following the standard approach of the uncertainty propagation.[37, 40, 44]

3.2 WZ CdSe Nanoribbons

To study the phase dependence of thermal conductivity of the ZB and WZ CdSe, we also measured two WZ CdSe nanoribbons (WZ1 and WZ2), and thermal conductivity results are given in Fig. 4(b). Sample WZ1 has a width of 352 nm and a thickness of 172 nm, and sample WZ2 is 330 nm in width and 174 nm in thickness. As seen in Fig. 4(b), effective thermal conductivity of sample WZ1 and that of sample WZ2 overlapped with each other due to their similar dimensions. The uncertainty in effective thermal conductivity of samples WZ1 and WZ2 is estimated to be less than 0.5 W/m-K for temperatures above 100 K. Following the same procedure mentioned above and assuming that the contact thermal resistance per unit area between the WZ nanoribbon and the membrane is the same as that between the ZB nanowire and the membrane, contact thermal resistances are estimated to be 3.4×10^5 K/W for sample WZ1 and 3.7×10^5 K/W for sample WZ2, which are less than 1% of the measured thermal resistances of samples WZ1 and WZ2. The relatively small contact thermal resistance is also verified by thermal conductivity results of sample

WZ1 before and after the deposition of the Pt-C composite (Fig. 2(d) and 2(e)). As shown in Fig. 4(b), the measured effective thermal conductivity of sample WZ1 before and after the deposition of the Pt-C composite is almost the same, indicating negligible contact thermal resistance between sample WZ1 and membranes.

At 300 K, thermal conductivity of samples WZ1 and WZ2 is almost the same, around 3.6 W/m-K, which is much lower than the bulk thermal conductivity of the WZ CdSe, 9 W/m-K.[21, 22] As shown in Fig. 4(b), above 80 K, thermal conductivity of two WZ nanoribbons (WZ1 and WZ2) decreases substantially with the increase of temperature, which indicates that Umklapp scattering dominates thermal transport in this temperature range. A peak thermal conductivity is observed for WZ nanoribbons at ~80 K, which is higher than the temperature for the peak thermal conductivity of the bulk WZ CdSe (~20 K),[19] suggesting that boundary scattering still plays an important role in reducing thermal conductivity of samples WZ1 and WZ2. Therefore, the observed lower than bulk thermal conductivity of WZ nanoribbons might be partially due to boundary scattering.

3.3 Phase Dependence

Our experimental results show that thermal conductivity of the measured ZB CdSe nanowires/nanoribbons (ZB1-ZB4) is higher than that of the WZ CdSe nanoribbons (WZ1 and WZ2) at room temperature. It should be noticed that the effect of crystal phases on thermal conductivity of nanostructures could change and even reverse with

the decrease of the nanostructure size. It has been reported that thermal conductivity of the ZB GaAs nanowire is smaller than that of the WZ InAs nanowire of similar diameter even though the bulk thermal conductivity of GaAs is larger than that of InAs.[45] However, as seen from Table I and Fig. 4, even for a ZB CdSe nanowire with a diameter as small as 41 nm, the measured thermal conductivity at room temperature, which should be much lower than the bulk thermal conductivity of the ZB CdSe, is higher than the bulk thermal conductivity of the WZ CdSe reported in the literature, suggesting that the bulk ZB CdSe possesses a higher thermal conductivity than the WZ phase at room temperature.

The relatively higher thermal conductivity of the ZB phase can be qualitatively explained using the simple model proposed by Slack.[6] At temperatures not too far from the Debye temperature of a solid, thermal conductivity can be estimated by the Slack's equation

$$k = A\frac{M_a\theta_D^3\delta}{\gamma^2 T n^{2/3}}, \quad (1)$$

and A is defined as

$$A = \frac{2.43\times10^{-8}}{1-0.514/\gamma+0.228/\gamma^2}, \quad (2)$$

where γ is the Grüneisen constant which is a measure of the deviation of a crystal from harmonicity, M_a is the average atomic mass (95.68 amu for CdSe), θ_D is the Debye temperature, δ^3 is the volume per atom, T is the temperature, and n is the number of atoms per unit cell. It can be seen from Eqs. (1) and (2) that a solid with

a high θ_D, a small γ, and a small n will possess a high thermal conductivity. For the ZB CdSe, γ = 0.6, θ_D = 164 K, δ =3.06 Å, and n = 2 when thermal conductivity is 23 W/m-K at 300 K,[6] and γ could be even lower if thermal conductivity of the bulk ZB CdSe is higher than 23 W/m-K. For the WZ CdSe, δ = 3.04 Å which is very close to that of the ZB CdSe due to the similar density, θ_D = 181 K, and n = 4.[22] From the reported bulk thermal conductivity of the WZ CdSe at 300 K (9 W/m-K),[21, 22] we can estimate γ = 0.93 for the WZ CdSe by using Eqs. (1) and (2). Compared to the WZ phase, the ZB phase CdSe has smaller γ and n due to its simple cubic structure and thus could possess higher thermal conductivity.

Our result is different from previous experimental results for InAs nanowires in the literature which suggest identical thermal conductivity for the bulk ZB and WZ InAs crystals.[2] It is still unclear why different compounds exhibit different phase dependence for their thermal transport properties. Zhou *et al.* hypothesized that the phase dependence of thermal conductivity might be related to the difference between the c/a ratio of the WZ phase and the ideal value of $\sqrt{8/3}$ (=1.633).[2] In fact, the c/a ratios of the WZ InAs and the WZ CdSe are 1.6436 and 1.630, respectively,[46, 47] both of which are very close to the ideal ratio of 1.633. However, different phase dependence has been observed for thermal conductivity of these two compounds, indicating that some other parameters may play a significant role in determining the phase dependence of thermal conductivity. Recently, Togo *et al*. calculated lattice thermal conductivity of 33 compounds with both ZB and WZ phases including InAs

and CdSe by using the LBTE model.[4] Their LBTE model predicted a lattice thermal conductivity of 25.3 W/m-K for the bulk ZB InAs and 18.6 W/m-K for the bulk thermal conductivity of the WZ InAs at 300 K. For CdSe, they predicted a thermal conductivity of 12.4 W/m-K for the ZB phase and a value of 8.81 W/m-K for the WZ phase at 300 K. Although higher thermal conductivity values are predicted for the ZB phase of both InAs and CdSe, Togo *et al*. regarded thermal conductivity values of ZB and WZ phases as similar and did not discuss the underlying mechanism causing the difference between thermal conductivity values of these two phases. In addition, in this work, we measured a thermal conductivity of 18.8 W/m-K at 300 K for a ZB nanoribbon (ZB4), which is higher than the bulk thermal conductivity of the ZB CdSe predicted by Togo *et al*. (12.4 W/m-K). As mentioned above, we expect that thermal conductivity of the bulk ZB CdSe could be even higher than 23 W/m-K at room temperature. The discrepancy between our experimental results and the prediction of the LBTE model is currently not understood yet and worth further studies.

4. Conclusions

In summary, we have measured thermal conductivity of CdSe nanostructures with both ZB and WZ phases. At room temperature, the measured thermal conductivity of the ZB CdSe nanowires with a diameter as small as 41 nm is higher than the bulk thermal conductivity of the WZ CdSe reported in the literature. Our study suggests that the bulk thermal conductivity of the ZB CdSe is higher than the WZ phase. The relatively higher thermal conductivity of the ZB phase can be explained by using the

Slack model considering that the ZB CdSe has smaller γ and n due to its simple cubic structure. Our result is different from experimental results for InAs nanowires in the literature which suggest similar thermal conductivity for both ZB and WZ phases.

Acknowledgments

The authors acknowledge the financial support from the National Natural Science Foundation of China (51176032, 51276153), Research Project of State Key Laboratory of Mechanical System and Vibration (MSV201413), and the Fundamental Research Funds for the Central Universities. D. X. acknowledges the financial support from the Research Grants Council of the Hong Kong Special Administrative Region, China, under Theme-based Research Scheme (Project No. T23-407/13-N).

Notes and References

1. C.-Y. Yeh, Z. W. Lu, S. Froyen and A. Zunger, *Phys. Rev. B*, 1992, **46**, 10086--10097.
2. F. Zhou, A. L. Moore, J. Bolinsson, A. Persson, L. Fröberg, M. T. Pettes, H. Kong, L. Rabenberg, P. Caroff, D. A. Stewart, N. Mingo, K. A. Dick, L. Samuelson, H. Linke and L. Shi, *Phys. Rev. B*, 2011, **83**, 205416.
3. W. Li and N. Mingo, *J. Appl. Phys.*, 2013, **114**, 183505.
4. A. Togo, L. Chaput and I. Tanaka, *Phys. Rev. B*, 2015, **91**, 094306.
5. A. AlShaikhi and G. P. Srivastava, *Phys. Rev. B*, 2007, **76**, 195205.
6. D. T. Morelli and G. A. Slack, in *High Thermal Conductivity Materials*, eds. S. L. Shinde and J. S. Goela, Springer, 2006.
7. D. K. Kim, Y. Lai, B. T. Diroll, C. B. Murray and C. R. Kagan, *Nat Commun*, 2012, **3**, 1216.
8. Y.-J. Doh, K. N. Maher, L. Ouyang, C. L. Yu, H. Park and J. Park, *Nano Lett.*, 2008, **8**, 4552-4556.
9. T. Ayvazian, W. E. van der Veer, W. Xing, W. Yan and R. M. Penner, *ACS Nano*, 2013, **7**, 9469-9479.
10. I. Gur, N. A. Fromer, M. L. Geier and A. P. Alivisatos, *Science*, 2005, **310**, 462-465.
11. W. U. Huynh, J. J. Dittmer and A. P. Alivisatos, *Science*, 2002, **295**, 2425-2427.
12. J. Li, C. Meng, Y. Liu, X. Wu, Y. Lu, Y. Ye, L. Dai, L. Tong, X. Liu and Q. Yang, *Adv. Mater.*, 2013, **25**, 833-837.
13. F. Xiao, K. Liu, Y. Bie, J. Zhao and F. Wang, *Appl. Phys. Lett.*, 2012, **101**, 093106.
14. A. Myalitsin, C. Strelow, Z. Wang, Z. Li, T. Kipp and A. Mews, *ACS Nano*, 2011, **5**, 7920-7927.
15. F. Vietmeyer, T. Tchelidze, V. Tsou, B. Janko and M. Kuno, *ACS Nano*, 2012, **6**, 9133-9140.
16. S. Schäfer, Z. Wang, T. Kipp and A. Mews, *Phys. Rev. Lett.*, 2011, **107**, 137403.
17. L. Dong, S. Niu, C. Pan, R. Yu, Y. Zhang and Z. L. Wang, *Adv. Mater.*, 2012, **24**, 5470-5475.
18. Z. Hu, X. Zhang, C. Xie, C. Wu, X. Zhang, L. Bian, Y. Wu, L. Wang, Y. Zhang and J. Jie, *Nanoscale*, 2011, **3**, 4798-4803.
19. P. L. Jacobs and R. K. Irey, Iowa State University, Ames, Iowa, 1969.
20. J. D. Beasley, *Appl. Opt.*, 1994, **33**, 1000-1003.
21. J. P. Feser, E. M. Chan, A. Majumdar, R. A. Segalman and J. J. Urban, *Nano Lett.*, 2013, **13**, 2122-2127.
22. G. A. Slack, *Phys. Rev. B*, 1972, **6**, 3791-3800.
23. N. Samarth, H. Luo, J. K. Furdyna, S. B. Qadri, Y. R. Lee, A. K. Ramdas and N. Otsuka, *Appl. Phys. Lett.*, 1989, **54**, 2680-2682.
24. W.-L. Ong, S. M. Rupich, D. V. Talapin, A. J. H. McGaughey and J. A. Malen,

Nat Mater, 2013, **12**, 410-415.
25. Y. Ma, M. Liu, A. Jaber and R. Y. Wang, *Journal of Materials Chemistry A*, 2015, **3**, 13483-13491.
26. P. Kim, L. Shi, A. Majumdar and P. L. McEuen, *Phys. Rev. Lett.*, 2001, **87**, 215502.
27. L. Shi, D. Li, C. Yu, W. Jang, D. Kim, Z. Yao, P. Kim and A. Majumdar, *J. Heat Transf.*, 2003, **125**, 881-888.
28. J. Yang, S. Waltermire, Y. Chen, A. A. Zinn, T. T. Xu and D. Li, *Appl. Phys. Lett.*, 2010, **96**, 023109.
29. J. Yang, Y. Yang, S. W. Waltermire, X. Wu, H. Zhang, T. Gutu, Y. Jiang, Y. Chen, A. A. Zinn, R. Prasher, T. T. Xu and D. Li, *Nat. Nanotechnol.*, 2012, **7**, 91-95.
30. A. Mavrokefalos, M. T. Pettes, F. Zhou and L. Shi, *Rev. Sci. Instrum.*, 2007, **78**, 034901.
31. H. Tang, X. Wang, Y. Xiong, Y. Zhao, Y. Zhang, Y. Zhang, J. Yang and D. Xu, *Nanoscale*, 2015, **7**, 6683-6690.
32. D. Li, Y. Wu, P. Kim, L. Shi, P. Yang and A. Majumdar, *Appl. Phys. Lett.*, 2003, **83**, 2934-2936.
33. K. Davami, A. Weathers, N. Kheirabi, B. Mortazavi, M. T. Pettes, L. Shi, J.-S. Lee and M. Meyyappan, *J. Appl. Phys.*, 2013, **114**, 134314.
34. A. L. Moore and L. Shi, *Meas. Sci. Technol.*, 2011, **22**, 015103.
35. M. C. Wingert, Z. C. Y. Chen, S. Kwon, J. Xiang and R. Chen, *Rev. Sci. Instrum.*, 2012, **83**, 024901.
36. A. Weathers, K. Bi, M. T. Pettes and L. Shi, *Rev. Sci. Instrum.*, 2013, **84**, 084903-084908.
37. J. Yang, Y. Yang, S. W. Waltermire, T. Gutu, A. A. Zinn, T. T. Xu, Y. Chen and D. Li, *Small*, 2011, **7**, 2334-2340.
38. C. W. Chang, D. Okawa, H. Garcia, A. Majumdar and A. Zettl, *Phys. Rev. Lett.*, 2007, **99**, 045901.
39. M. Liangruksa and I. K. Puri, *J. Appl. Phys.*, 2011, **109**, 113501.
40. C. Yu, S. Saha, J. Zhou, L. Shi, A. M. Cassell, B. A. Cruden, Q. Ngo and J. Li, *J. Heat Transf.*, 2006, **128**, 234-239.
41. R. Prasher, *Phys. Rev. B*, 2008, **77**, 075424.
42. E. Rabani, *J. Chem. Phys.*, 2002, **116**, 258-262.
43. W.-X. Zhou, K.-Q. Chen, L.-M. Tang and L.-J. Yao, *Phys. Lett. A*, 2013, **377**, 3144-3147.
44. H. W. Coleman and W. G. Steele, *Experimentation and Uncertainty Analysis for Engineers*, John Wiley & Sons Inc., New York, NY, 2nd edn., 1999.
45. Y.-Y. Liu, W.-X. Zhou, L.-M. Tang and K.-Q. Chen, *Appl. Phys. Lett.*, 2013, **103**, 263118.
46. D. Kriegner, C. Panse, B. Mandl, K. A. Dick, M. Keplinger, J. M. Persson, P. Caroff, D. Ercolani, L. Sorba, F. Bechstedt, J. Stangl and G. Bauer, *Nano Lett.*, 2011, **11**, 1483-1489.
47. O. Madelung, *Semiconductors: Data Handbook*, Springer, Berlin, 2004.

Figure Captions

Figure 1 HRTEM images of CdSe nanostructures measured in this work. (a) A CdSe nanowire with the ZB phase (sample ZB1). The HRTEM image and the electron diffraction pattern in the inset confirm that the ZB nanowire grows along <110> direction. (b) A WZ CdSe nanoribbon (sample WZ1). The growth direction is [001].

Figure 2 SEM images of CdSe samples. (a), (b), and (c) show sample ZB1 which was measured three times with suspended lengths of 8.7 μm, 3.7 μm, and 3.7 μm (with the Pt-C composite), respectively. (d) and (e) show sample WZ1 which was measured before and after the deposition of the Pt-C composite, respectively.

Figure 3 (a) Effective thermal conductivity and intrinsic thermal conductivity obtained for sample ZB1. (b) Contact thermal resistance between sample ZB1 and two membranes.

Figure 4 Thermal conductivity of CdSe nanostructures. (a) ZB phase nanowires/nanoribbons. The diameters of sample ZB1, ZB2, and ZB3 are 52 nm, 41 nm, and 88 nm, respectively. Sample ZB4 is a nanoribbon with a width of 485 nm and a thickness of 195 nm; (b) WZ phase nanoribbons. Sample WZ1 has a width of 352 nm and a thickness of 172 nm, and sample WZ2 is 330 nm wide and 174 nm

thick. The bulk thermal conductivity of the WZ CdSe is taken from the literature,[19] and the orientation is [0001].

Figure 1, Yang *et al*.

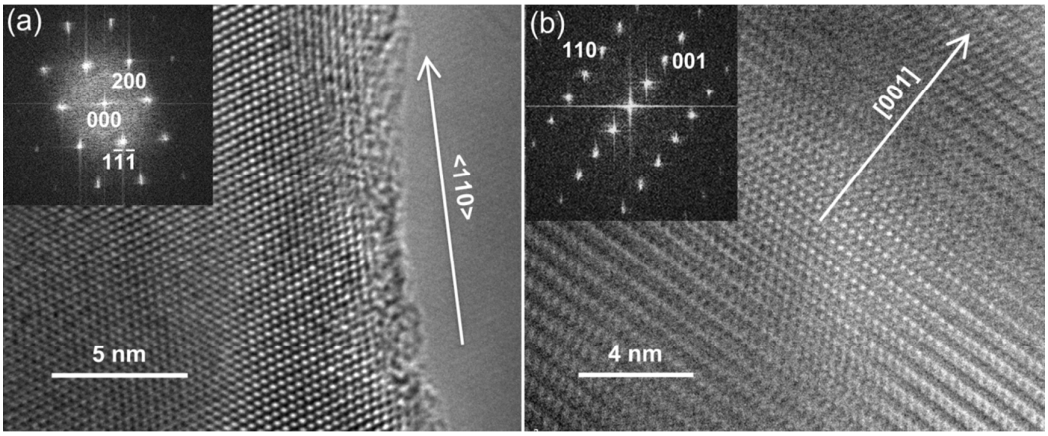

Figure 2, Yang *et al*.

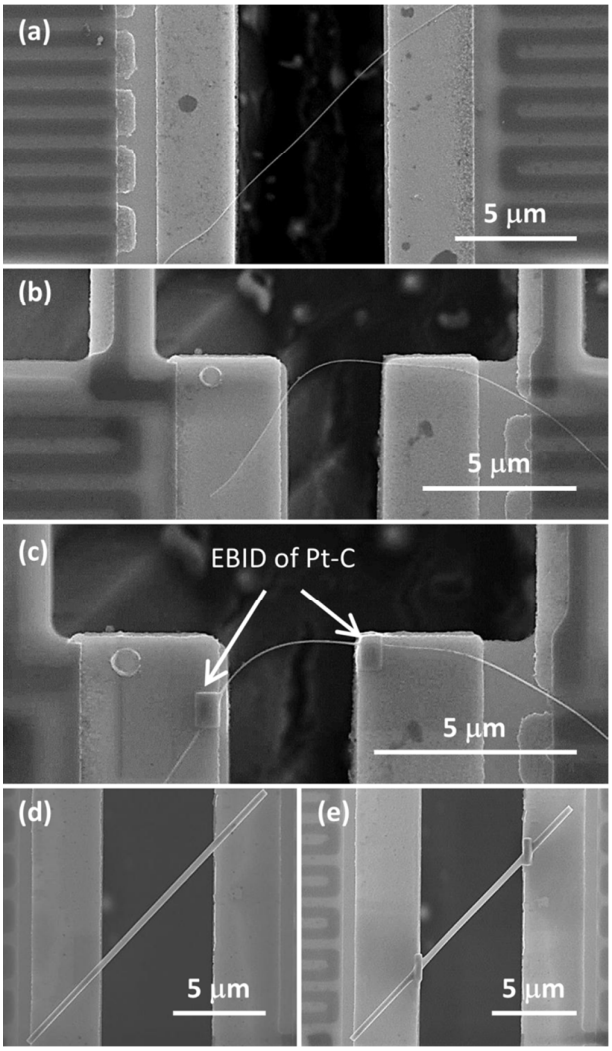

Figure 3, Yang *et al*.

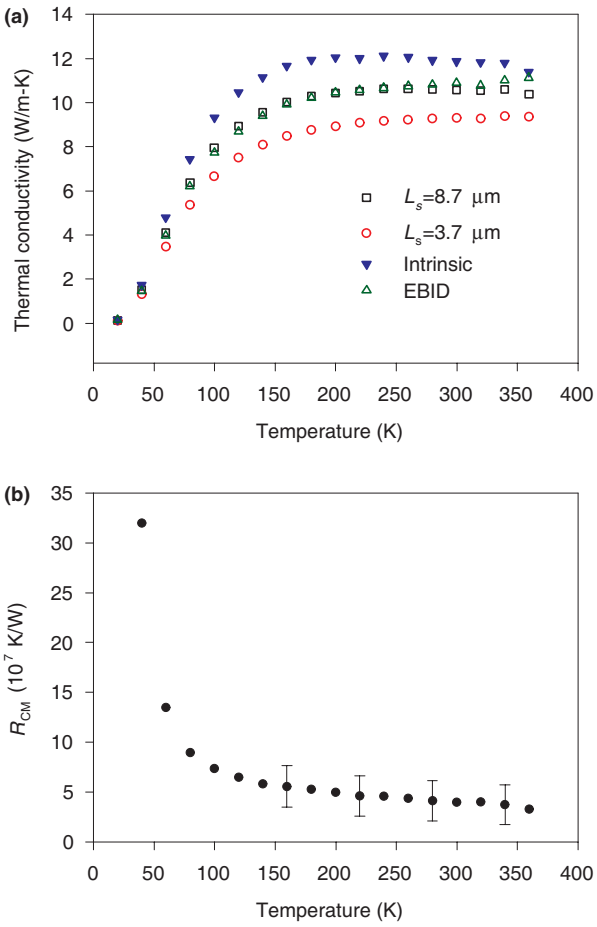

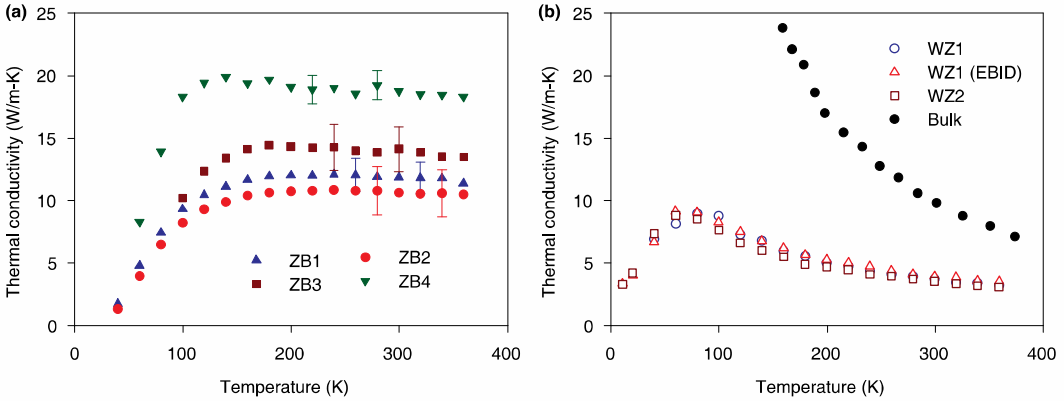

Table I. Summary of the measured CdSe nanostructures. *k* is the measured thermal conductivity at 300 K. Samples ZB1-ZB3 are nanowires (NW) and the lateral dimension in the table refers to the diameter. Samples ZB4, WZ1, and WZ2 are nanoribbons (NR) and the two lateral dimensions refer to the width and thickness of the nanoribbon.

Label	Phase	Lateral Dimension(s)	Growth Direction	*k* (W/m-K)
ZB1	Zinc blende	52 nm (NW)	<110>	11.9
ZB2	Zinc blende	41 nm (NW)	<110>	10.6
ZB3	Zinc blende	88 nm (NW)	<110>	14.1
ZB4	Zinc blende	485 nm×195 nm (NR)	<100>	18.8
WZ1	Wurtzite	352 nm×172 nm (NR)	[001]	3.6
WZ2	Wurtzite	330 nm×174 nm (NR)	[001]	3.6